Modelling the Study of Hand, Foot and Mouth Disease Using SVEIQAR Derived Model

Putsadee Pornphol[1], Porpattama Hammachukiattikul[2], Rajarathinam Vadivel[2], Emmanuel Sabastine[3], Saratha Sathasivam[4,*]

[1] Department of Digital Technology, Faculty of Science and Technology, Phuket Rajabhat University, Phuket 83000, Thailand
[2] Department of Mathematics, Faculty of Science and Technology, Phuket Rajabhat University, Phuket 83000, Thailand
[3] Department of Mathematical Sciences Federal University Lokoja, Kogi State Nigeria
[4] School Mathematical Sciences, Universiti Sains Malaysia, Penang, 11800, USM, Malaysia

ARTICLE INFO	ABSTRACT
   	This study introduces a mathematical model aimed at investigating the intricate dynamics of infectious diseases, incorporating vaccination and quarantine interventions. The model comprises a system of ordinary differential equations that delineate interactions among susceptible, infected, and recovered individuals, alongside the impacts of vaccination and quarantine measures. The disease transmission rate is contingent on the count of infected, asymptomatic, and quarantined individuals. The model undergoes a comprehensive analysis to ascertain pivotal equilibrium points—disease-free and endemic. Additionally, the stability of these equilibria is rigorously examined to discern their resilience in the presence of interventions. Furthermore, the model serves as a strategic tool for crafting effective disease control strategies. The study underscores the potential potency of synergistic vaccination and quarantine interventions by minimising infection rates. Employing sophisticated numerical optimization techniques, the study tackles the equations' complexity. The findings underscore the substantive impact of coordinated vaccination and quarantine strategies in curtailing disease spread. These insights furnish policymakers and health authorities with empirically grounded methodologies to formulate robust responses to infections such as hand, foot, and mouth diseases. Ultimately, this research contributes to the armamentarium of tools that empower the formulation of effective strategies to safeguard public health.

1. Introduction

Hand, foot, and mouth disease (HFMD) is a viral illness that primarily affects young children. It is caused by a group of viruses known as enteroviruses, most commonly the coxsackievirus A16 and enterovirus 71. The disease is typically characterized by a fever, sore throat, and painful sores or blisters on the hands, feet, and mouth, sometimes on the buttocks. It is highly contagious and can spread quickly among children in daycare or school settings [1,2]. The first known outbreak of HFMD

---

* *Corresponding author.*
E-mail address: saratha@usm.my

occurred in Toronto, Canada in 1957. Since then, numerous outbreaks have been reported worldwide. Several studies have been conducted to understand the epidemiology, clinical features, and management of HFMD [3,4]. A study conducted in Singapore found that enterovirus 71 was responsible for more severe cases of HMFD, with a higher risk of neurological complications such as meningitis and encephalitis. Another study [5] in China found that the incidence of HMFD was highest in children under the age of five and that outbreaks were more common during the summer and fall months. There is currently no specific antiviral treatment for HMFD. Prevention measures include good hand hygiene and avoiding close contact with infected individuals. overall HFMD remains an important public health concern, particularly in countries with high population densities and limited healthcare resources. Continued research into epidemiology and management is needed to reduce the burden of this disease on children and their families. The outbreak of HFMD typically occurs in the summer and fall months [6,7]. During epidemics of HFMD, it is recommended that patients be either hospitalized or quarantined at home, as the virus can spread rapidly through various modes of transmission, including aerosols, ingestion, and contact with contaminated objects [8]. This precaution is taken to minimize direct contact with infected individuals. HFMD has also created significant social and economic challenges, leading to the closure of schools and other public places and disruptions to parents' work and childcare arrangements. While efforts are made to encourage parents to keep their children away from public areas during outbreaks, additional societal and economic issues arise during disease outbreaks, which are difficult to quantify [9].

Mathematical models have been extensively used to study the transmission dynamics of infectious diseases, and have been instrumental in the development of control strategies. Various models have been developed, ranging from simple compartmental models to more complex individual-based models.

The SIR (Susceptible-Infected-Recovered) model is one of the most well-known and widely used models for infectious disease transmission. In recent years, several studies have incorporated the effects of vaccination and quarantine into infectious disease models. Vaccination is a highly effective intervention in reducing the spread of infectious diseases and has been widely used in controlling outbreaks. Quarantine, on the other hand, has been used to restrict the movement of individuals who have been exposed to an infectious disease, to prevent further transmission [9].

Another study by Gerardo *et al.,* [10] investigated the effectiveness of quarantine in controlling the spread of Ebola virus disease in West Africa. The study found that the implementation of quarantine was an effective intervention in reducing the number of cases.

In summary, the incorporation of vaccination and quarantine into infectious disease models has become increasingly important in the development of effective control strategies. In this work, we present a mathematical model for the transmission dynamics of a hypothetical infectious disease (HFMD), which includes the effects of vaccination and quarantine, to derive the model equations and analyse the properties of the model, to study the impact of vaccination, quarantine interventions and trend of the infection on disease transmission dynamics.

The organization of this work is as follows:

i. Chapter 1 provides an introduction to the study of infectious disease transmission dynamics and the use of mathematical models in disease control.

ii.   Chapter 2 presents the model diagram and equations for the transmission dynamics of an infectious disease with vaccination and quarantine interventions. The properties of the model are analysed, and the endemic equilibrium is derived.

iii.   Chapter 3 discusses the mathematical model analysis, the reproduction number and the local stability of the disease-free equilibrium of the model.

iv.   Chapter 4 presents the global stability of disease-free equilibrium, endemic equilibrium point, estimation of the model parameters using data fitting, bifurcation analysis of the model and showing the impact of vaccination and quarantine interventions on disease transmission dynamics.

v.   Chapter 5 summarizes the main findings of the study and provides recommendations for future research.

2. Methodology

HFMD is a viral infection that primarily affects young infants, making them more vulnerable to the disease. This puts them at risk of spreading the virus quickly, potentially leading to a widespread outbreak. The disease is most contagious within the first week of symptoms appearing, and initial symptoms include fever, sore throat, reduced appetite, and malaise. Within a short time, the person affected will develop painful blisters in the mouth and on the hands, feet, and other areas of the body [11,12]. These blisters eventually break and form ulcers. Once the fever and rash subside, the patient is considered to have clinically recovered from HFMD.

2.1 Introduction

In an attempt to stop the spread of HFMD, the SIR concept was explored in Sarawak [12]. However, the model only showed good accuracy when real data was pushed one week ahead, making it difficult to convincingly demonstrate its ability to forecast the actual infectious behaviour. To improve prediction accuracy, a new mathematical model called SVEQIAR was developed by including compartments for the vaccinated group, quarantine, and the asymptomatic group. MATLAB simulations were used to compare the new model with the earlier SEIPR model. The study aimed to describe the disease's quantitative behaviour by incorporating the vaccinated, asymptomatic, and quarantine groups in the model. This model of compartments is displayed. The parameters are:

i.   Susceptible (S): Individuals who are not infected with HFMD and are susceptible to the virus.

ii.   Exposed (E): Individuals who have been exposed to the virus and are in the latent period of infection during which they are infected but not yet infectious themselves.

iii.   Infected (I): Individuals who have been infected with the virus and are infectious and display symptoms.

iv.   Quarantine (Q): Individuals who have been quarantined with the virus and are experiencing severe symptoms such as meningitis, encephalitis or acute flaccid paralysis.

v.   Asymptomatic (A): Individuals who have been infected with the virus, were asymptomatic and have recovered from the infection.

vi.   Vaccinated (V) is the number of individuals who have been vaccinated against the disease.

vii. α Natural birth rate.

viii.   μ: Natural death rate.

  ix. θ: Proportion of individuals that move from exposure to infectious.

  x. ω: Rate of vaccine coverage at which a clinically recovered individual fully recovers per unit of time.

  xi. γ: Proportion of infected individuals that are clinically recovered.

  xii. π: Rate at which a recovered individual loses its immunity.

  xiii. δ: Death rate caused by the disease.

  xiv. β: Transmission rate of the disease.

  xv. τ: Scaling factor of the vaccine efficacy.

  xvi. D_1: Modification parameter associated with asymptomatic individuals.

  xvii. D_2: Modification parameter associated with quarantined individuals.

  xviii. K: Rate at which infected individuals recover.

  xix. ε: Rate at which quarantined individuals recover.

  The diagram presented (Figure 1) along with the subsequent set of differential equations illustrate how individuals transition between various compartments.
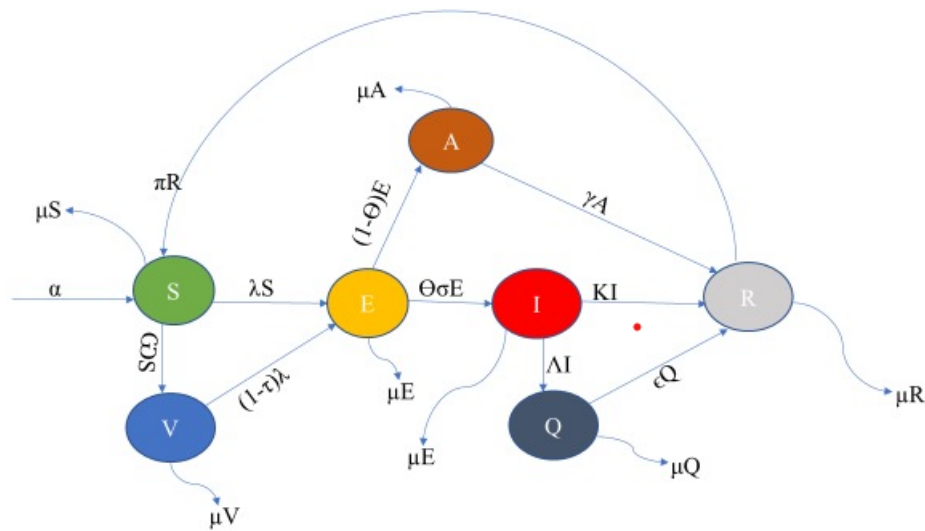

Fig. 1. Flow of Individual Between Compartment

$$\frac{dS}{dt} = \alpha + \pi R - (\lambda + \omega + \mu)S = f_1 \tag{1}$$

$$\frac{dV}{dt} = \omega S - ((1 - \tau)\lambda + \mu)V = f_2 \tag{2}$$

$$\frac{dE}{dt} = \lambda S + (1 - \tau)\lambda V - (\sigma + \mu)E = f_3 \tag{3}$$

$$\frac{dI}{dt} = \theta\sigma E - (K + \omega + \delta + \mu)I = f_4 \tag{4}$$

$$\frac{dA}{dt} = (1 - \theta)\sigma E - (\gamma + \delta + \mu)A = f_5 \tag{5}$$

$$\frac{dQ}{dt} = \omega I - (\varepsilon + \delta + \mu)Q = f_6 \tag{6}$$

$$\frac{dR}{dt} = KI + \gamma A + \varepsilon Q - (\pi + \mu)R = f_7 \tag{7}$$

2.2 Mathematical Model Analysis
2.2.1 Disease-free equilibrium

At the disease-free equilibrium (DFE), when $E = I = A = Q = 0$, it follows that $R = 0$. The equilibrium values are given by:

$$S^* = \frac{\alpha}{(\omega + \mu)} \tag{8}$$

$$V^* = \frac{\alpha\omega}{(\mu(\omega + \mu))} \tag{9}$$

The equilibrium state is:

$$(S^*, V^*, E^*, I^*, A^*, Q^*, R^*) = \left(\frac{\alpha}{(\omega + \mu)}, \frac{\alpha\omega}{(\mu(\omega + \mu))}, 0, 0, 0, 0, 0\right) \tag{10}$$

2.3 Reproduction Number

Let

$$\lambda = \beta(I + D_1 A + D_2 Q). \tag{11}$$

The column vector of the infected class of Eq. (3) to Eq. (6) is given as:

$$F = [\beta(I + D_1 A + D_2 Q)S + (1 - \tau)\beta(I + D_1 A + D_2 Q)V, 0, 0, 0]^{\mathrm{T}} \tag{12}$$

Differentiating F partially with respect to E, I, A, Q

$$\begin{pmatrix} 0 & \beta(S + (1 - \tau)V) & D_1\beta(S + (1 - \tau))V & D_2\beta(S + (1 - \tau))V \\ 0 & 0 & 0 & 0 \\ 0 & 0 & 0 & 0 \\ 0 & 0 & 0 & 0 \end{pmatrix} \tag{13}$$

$$\nabla F = \begin{pmatrix} 0 & \frac{\beta\alpha(\mu+(1-\tau)\omega)}{\mu(\omega+\mu)} & \frac{\beta D_1\alpha(\mu+(1-\tau)\omega)}{\mu(\omega+\mu)} & \frac{\beta D_2\alpha(\mu+(1-\tau)\omega)}{\mu(\omega+\mu)} \\ 0 & 0 & 0 & 0 \\ 0 & 0 & 0 & 0 \\ 0 & 0 & 0 & 0 \end{pmatrix} \tag{14}$$

Let $A_1 = \frac{\beta\alpha(\mu+(1-\tau)\omega)}{\mu(\omega+\mu)}$, $A_2 = \frac{\beta D_1\alpha(\mu+(1-\tau)\omega)}{\mu(\omega+\mu)}$ and $A_3 = \frac{\beta D_2\alpha(\mu+(1-\tau)\omega)}{\mu(\omega+\mu)}$
Also, from the infected model equation, we have

$$v = \begin{pmatrix} (\delta + \mu)E \\ (K + \Lambda + \delta + \mu)I - \theta\sigma E \\ (\gamma + \delta + \mu)A - (1 - \theta)\sigma E \\ (\epsilon + \delta + \mu)Q - \Lambda I \end{pmatrix}$$

(15)

$$\nabla v = \begin{pmatrix} (\delta + \mu) & 0 & 0 & 0 \\ -\theta\sigma & (K + \Lambda + \delta + \mu) & 0 & 0 \\ -(1 - \theta)\sigma & 0 & (\gamma + \delta + \mu) & 0 \\ 0 & -\Lambda & 0 & (\epsilon + \delta + \mu) \end{pmatrix}$$

(16)

We obtained the eigen values from the matrix's relation $|F * \nabla v - \lambda I| = 0$, we have $\lambda_1 = \lambda_2 = \lambda_3 = 0$ and $\lambda_4 =$ The Reproduction Number, obtained as

$$R_0 = \frac{D_0}{(\mu\,(\omega + \mu)(\sigma + \mu)(K + \omega + \delta + \mu)(\gamma + \delta + \mu)(\epsilon + \delta + \mu))}$$

(17)

where

$$D_0 = \beta\,\alpha\,\sigma\,(\mu + (1 - \tau)\,\omega) * ((\theta\,(\gamma + \delta + \mu)) * (D_2\,\omega + \varepsilon + \delta + \mu) + D_1\,(1 - \theta)\,(K + \omega + \delta + \mu)\,(\varepsilon + \delta + \mu))$$

(18)

2.4 Local Stability of Disease-Free Equilibrium

In mathematical modelling, local stability refers to the behaviour of a system in the vicinity of an equilibrium point. An equilibrium point is a point where the values of the variables do not change over time. Local stability analysis is important in determining the behaviour of a system in the long term.

To determine the local stability of the system, we need to linearize the system about an equilibrium point and examine the eigenvalues of the resulting Jacobian matrix. Let $(S^*, V^*, E^*, I^*, A^*, Q^*, R^*)$ be an equilibrium point of the system, i.e., a point where all the derivatives are zero. We then compute the Jacobian matrix J at this equilibrium point by computing the partial derivatives of each equation with respect to each variable and evaluating them at $(S^*, V^*, E^*, I^*, A^*, Q^*, R^*)$

$$\begin{bmatrix} -(\omega + \mu) & 0 & 0 & \frac{-\beta\alpha}{(\omega+\mu)} & \frac{-\beta D_1\alpha}{(\omega+\mu)} & \frac{-\beta D_2\alpha}{(\omega+\mu)} & \pi \\ \omega & -\mu & 0 & \frac{-\beta(1-\tau)\alpha\omega}{\mu(\omega+\mu)} & \frac{-\beta D_1(1-\tau)\alpha\omega}{\mu(\omega+\mu)} & \frac{-\beta D_2(1-\tau)\alpha\omega}{\mu(\omega+\mu)} & 0 \\ 0 & 0 & -(\sigma + \mu) & \frac{\beta\alpha(\mu+(1-\tau)\omega)}{\mu(\omega+\mu)} & \frac{\beta\alpha D_1(\mu+(1-\tau)\omega)}{\mu(\omega+\mu)} & \frac{\beta\alpha D_2(\mu+(1-\tau)\omega)}{\mu(\omega+\mu)} & 0 \\ 0 & 0 & \theta\sigma & -(K + \Lambda + \delta + \mu) & 0 & 0 & 0 \\ 0 & 0 & (1-\theta)\sigma & 0 & -(\gamma + \delta + \mu) & 0 & 0 \\ 0 & 0 & 0 & \Lambda & 0 & -(\epsilon + \delta + \mu) & 0 \\ 0 & 0 & 0 & K & \gamma & \epsilon & -(\pi + \mu) \end{bmatrix}$$

$$= \begin{bmatrix} -C_1 & 0 & 0 & -C_4 & -C_8 & -C_{12} & \pi \\ \omega & -\mu & 0 & -C_5 & -C_9 & -C_{13} & 0 \\ 0 & 0 & -C_2 & C_6 & C_{10} & C_{14} & 0 \\ 0 & 0 & \theta\sigma & -C_7 & 0 & 0 & 0 \\ 0 & 0 & C_3 & 0 & -C_{11} & 0 & 0 \\ 0 & 0 & 0 & \Lambda & 0 & -C_{15} & 0 \\ 0 & 0 & 0 & K & \gamma & \epsilon & -C_{16} \end{bmatrix}$$

(19)

Then, we calculate the characteristic equation of the Jacobian matrix: $|J - \lambda I| = 0$ and obtained the following values of λ

$\lambda_1 = C_{11} = (\gamma + \delta + \mu)$, $\lambda_2 = -C_{16} = (\pi + \mu)$, $\lambda_2 = \mu$ and
$\lambda^4 + (C_2 + C_7 + C_{11} + C_{15})\lambda^3 + (C_2 C_7 + C_2 C_{11} + C_2 C_{15} - C_3 C_{10} + C_7 C_{11} + C_7 C_{15} + C_{11} C_{15} - (\theta \sigma C_6 + C_3 C_{10}))\lambda^2 + (C_2 C_{11} C_7 + C_2 C_7 C_{15} + C_2 C_{11} C_{15} + C_7 C_{11} C_{15} - (\theta \sigma C_{14} + \theta \sigma C_6 C_{11} + \theta \sigma C_6 C_{15} + C_3 C_{10} C_{10} + C_3 C_{10} C_{15}))\lambda - (\theta \sigma C_{14} C_{11} + \theta \sigma C_6 C_{11} C_{15} + C_3 C_7 C_{10} C_{15}) = 0$

The above equation can be started as

$$b_4 \lambda^4 + b_3 \lambda^3 + b_2 \lambda^2 + b_1 \lambda + b_0 = 0 \tag{20}$$

We use Routh-Hurwitz criterion [13] which stipulate that all polynomial roots have a negative real component if and only if the coefficients a_i are positive and the determinant of the matrices $H_i > 0$ for $i = 0,1,2,3,4$ thus,

$$H_1 = 1 = b_1 + b_2 + b_3 + b_4 > 0 \tag{21}$$

$$H_2 = \begin{bmatrix} b_3 & b_1 \\ 1 & b_2 \end{bmatrix} = b_3 b_2 - b_1 > 0 \; iff \; b_3 b_2 > b_1 \tag{22}$$

$$H_3 = \begin{bmatrix} b_3 & b_1 & 0 \\ 1 & b_2 & b_0 \\ 0 & b_3 & b_1 \end{bmatrix} = b_3 \begin{bmatrix} b_2 & b_0 \\ b_3 & b_1 \end{bmatrix} - b_1 \begin{bmatrix} 1 & b_0 \\ 0 & b_1 \end{bmatrix} = b_3(b_1 b_2 - b_0 b_3) - b_1^2$$

$$H_3 = b_1 b_2 b_3 - (b_0 b_3^2 + b_1^2) > 0 \; iff \; b_1 b_2 b_3 > b_0 b_3^2 + b_1^2 \tag{23}$$

$$H_4 = \begin{bmatrix} b_3 & b_1 & 0 & 0 \\ 1 & b_2 & b_0 & 0 \\ 0 & b_3 & b_1 & 0 \\ 0 & 1 & b_2 & b_0 \end{bmatrix} = b_3[b_0 b_1 b_2 - b_3 b_0^2] - b_1(b_0 b_1)$$

$$= b_0 b_1 b_2 b_3 - (b_0 b_1^2 + b_0^2 b_3^2) > 0 \; iff \; b_0 b_1 b_2 b_3 > (b_0 b_1^2 + b_0^2 b_3^2) \tag{24}$$

Therefore, all the eigen values of the polynomial have negative real parts, implying that $\lambda_i < 0$, for $i = 1,2,3,4$ when $R_0 < 1$, we conclude that the disease-free equilibrium point is locally asymptotically stable.

2.5 Global Stability of the Disease-Free Equilibrium

Using the Castilo-Chavez conditions in [14], we examine the global asymptotic stability of the disease-free equilibrium for the model Eq. (1) to Eq. (7).

Lemma 1: Consider a sample system that takes the form

$$
\left.\begin{array}{l}
\frac{dX}{dt} = F(X,Y) \\
\frac{dY}{dt} = G(X,Y), (X,0)
\end{array}\right\} \tag{25}
$$

Where $X = \{S, V, R\}$ and $Y = \{E, I, A, Q\}$ with the components $X \in R^3$ signifying the population that is unaffected and the population $Y \in R^4$ that is sick. The current notation for the disease-free state is $E_0 = (X^*, 0)$, where $X^* = \alpha/(\omega + \mu), \alpha\omega/(\mu(\omega + \mu))$.

To ensure worldwide asymptotic stability, the following requirements must be met. Suppose that,

$H_1: dX/dt = F(X^*, 0), X^*$ is globally asymptotically stable;

$H_2: G(X,Y) = PY - G(X,Y), G(X,Y) \geq 0$ for $(X,Y) \in \Gamma$

Where $P = D_z G(X^*, 0)$ is an N-matrix (the off-diagonal elements of P are non-negative) and Γ the area where the concepts make biological sense. If so then E_0, is guaranteed to be globally asymptotically steady provided that $R_0 < 1$ (Castillo-Chavez *et al.,*).

Theorem 1:

The model Eq. (1) to Eq. (7) at the point $(X^*, 0)$ is globally asymptotically stable provided that $R_0 < 1$ and H_1, H_2 hold.

Proof

We need to show that the conditions H_1 and H_2 hold when $R_0 < 1$. From our model Eq. (1) to Eq. (7) we have, for the group that is not infected

$$
F(X,0) = \begin{bmatrix} \alpha + \pi - (\lambda + \omega + \mu)S \\ \omega S - \lambda(1 - \tau\mu) \\ KI + \gamma A + \epsilon Q - (\pi + \mu)R \end{bmatrix} \tag{26}
$$

therefore $X^* = \left(\frac{\alpha}{\omega+\mu}, \frac{\alpha\omega}{\mu(\omega+\mu)}, 0\right)$ is asymptotically steady across the board. This can be demonstrated below,

$$
\begin{aligned}
S(t) &= \left(\frac{\alpha}{\omega+\mu} + \left(S(0) - \frac{\omega}{(\omega+\mu)}\right) exp^{-(\omega+\mu)t}\right) \\
V(t) &= \left(\frac{\alpha\omega}{\mu(\omega+\mu)} + \left(V(0) - \frac{\alpha\omega}{\mu(\omega+\mu)}\right) exp^{-(\omega+\mu)t}\right)
\end{aligned} \tag{27}
$$

$$R(t) = R(0)exp^{-\mu t}$$

As $t \to \infty, S \to \frac{\alpha}{\omega+\mu}, V \to \frac{\alpha\omega}{\mu(\omega+\mu)}, R \to 0$

Hence x^* convergence is global in Ω. Therefore $\left(\frac{\alpha}{\omega+\mu}, \frac{\alpha\omega}{\mu(\omega+\mu)}, 0\right)$ is globally asymptotically stable and satisfied H_1

The second condition of the theorem $G(X,Y) = PY - G(X,Y), G(X,Y) \geq 0$, where p is an $m \times m$ matrix, Y is a column vector formed from the infectious classes. Recalled

$$G(X,Y) = \begin{bmatrix} \lambda S + (1-\tau)\lambda V - (\sigma + \mu)E \\ \theta\sigma E - (K + \wedge + \delta + \mu)I \\ (1-\theta)\sigma E - (\gamma + \delta + \mu)A \\ \wedge I - (\epsilon + \delta + \mu)Q \end{bmatrix}, Y = \begin{bmatrix} E \\ I \\ A \\ Q \end{bmatrix} \text{ and}$$

$$P = \begin{bmatrix} -(\sigma + \mu) & 0 & 0 & 0 \\ \theta\sigma & -(K + \wedge + \delta + \mu) & 0 & 0 \\ (1-\theta)\sigma & 0 & -(\gamma + \delta + \mu) & 0 \\ 0 & \wedge & 0 & -(\epsilon + \delta + \mu) \end{bmatrix} \quad (28)$$

Thus

$$G_\wedge(X,Y) = \begin{bmatrix} -\lambda S - (1-\tau)\lambda V \\ 0 \\ 0 \\ 0 \end{bmatrix} \quad (29)$$

Since $G(X,Y) \leq 0$, H_2 is not fulfilled. It follows from this that E_0 may not be universally asymptotically stable when $R_0 < 1$, therefore the model may exhibit backward bifurcation.

2.6 Endemic Equilibrium Point (EEP)

To find the Endemic Equilibrium Point (EEP), we need to solve the system of equations for the values of $S^*, V^*, E^*, I^*, A^*, Q^*$ and R^*, that satisfy the condition that the time derivatives of $S^*, V^*, E^*, I^*, A^*, Q^*$ and R^* are all zero. This results in a set of equations that we solve simultaneously to obtain the values of $S^*, V^*, E^*, I^*, A^*, Q^*$ and R^* at the EEP. The EEP is also referred to as a steady state or a fixed point.
We obtain:

$$\left. \begin{array}{l} \alpha + \pi R - (\lambda + \omega + \mu)S = 0 \\ \omega S - ((1-\tau)\lambda + \mu)V = 0 \\ \lambda S + (1-\tau)\lambda V - (\sigma + \mu)E = 0 \\ \theta\sigma E - (K + \omega + \delta + \mu)I = 0 \\ (1-\theta)\sigma E - (\gamma + \delta + \mu)A = 0 \\ \omega I - (\varepsilon + \delta + \mu)Q = 0 \\ KI + \gamma A + \epsilon Q - (\pi + \mu)R = 0 \end{array} \right\} \quad (30)$$

Solving this system of equations, we obtained the values of the variables at the EEP, denoted by $S^*, V^*, E^*, I^*, A^*, Q^*$ R^*., Let $a_1 = \delta + \Lambda + K + \mu;\ a_3 = \varepsilon + \delta + \mu;\ a_4 = \gamma + \omega + \mu;$ $a_5 = \gamma + \omega + \mu;\ a_6 = \pi + \mu;\ a_6 = \gamma + \delta + \mu;\ a_7 = \varepsilon + \delta + \mu;$

$$E^* = \frac{(K + \wedge + \delta + \mu)I}{\theta\sigma} \quad (31)$$

$$I^* = \frac{\theta \sigma E^*}{K + \Lambda + \delta + \mu} \tag{32}$$

$$A^* = \frac{-(\theta - 1)(K + \Lambda + \delta + \mu)I}{\theta(\gamma + \delta + \mu)} \tag{33}$$

$$Q^* = \frac{(\Lambda I}{(\varepsilon + \delta + \mu)} \tag{34}$$

$$S^* = \frac{\pi I \gamma^2 a_1}{a_4 a_5 a_6 \theta} - \frac{\pi I \gamma a_1}{a_4 a_5 a_6} + \frac{\pi \Lambda I \epsilon}{a_4 a_5 a_7} + \frac{\pi K I}{a_4 a_5} + \frac{\alpha}{a_4} \tag{35}$$

$$V^* = \frac{-((\pi \, ((-K a_6 + \gamma \, a_1) \, \theta - \gamma \, a_1) \, a_6 - \theta \, \Lambda \, \varepsilon \, a_6 \, I - \alpha \, \theta \, a_5 \, a_6 \, a_7) \, \omega)}{(a_5 \, ((C a_1 - a_6) \, \theta \, a_7 - D \, \Lambda \, \theta \, a_6 \, (\tau - 1) \, I + \mu \, \theta \, a_6 \, a_7) \, a_4} \tag{36}$$

$$\lambda = \beta \left(\frac{(1 - \theta) a_1 I D_1}{\theta a_6} + \frac{D_2 \Lambda I}{a_7} + I \right) \tag{37}$$

$$R^* = \frac{K I^* + \gamma A^* + \epsilon Q}{\pi + \mu} \tag{38}$$

At EEP, we have $\frac{dE}{dt} = 0$, which gives $\frac{dE}{dt} = \lambda S + (1 - \tau)\lambda V - (\sigma + \mu)E = 0$.

Simplifying and expressing the equation in descending power of I we obtain the equation in form of

$$Z_1 I^3 + Z_2 I^2 + Z_3 I = 0$$
$$\Longrightarrow Z_1 I^2 + Z_2 I + Z_3 = 0 \tag{39}$$

Where Z_1 and Z_2 are coefficient of I^2 and I, obtained as

$$Z1 = \pi \, \beta^2 \sigma \, (-D_1 \theta \, a_1 a_7 + D_2 \, \Lambda \, \theta \, a_6 + -D_1 a_1 a_7 + \theta \, a_6 a_7)^2 (\tau - 1)(K \, \theta \, a_6 + \Lambda \, \varepsilon \, \theta \, a_6 + \gamma^2 a_1 a_7 - \gamma \, \theta \, a_1 a_7) \tag{40}$$

$$Z2 = -(((((-(\beta \, \alpha \, (\tau - 1) \, a5 - K \, \pi \, (\omega \, \tau - \mu - \omega)) \, a6 + (D1 \, \beta \, \alpha \, (\tau - 1) \, a5 + \pi \, \gamma \, (\omega \, \tau - \mu - \omega) \, a1)) \, \theta - (-a4 \, a5 \, (\tau - 1) \, a6 + D1 \, \beta \, \alpha \, (\tau - 1) \, a5 + \pi \, \gamma \, (-\gamma \, \mu + \omega \, \tau - \omega)) \, a1) \, \sigma + a1 \, a4 \, a5 \, a6 \, \mu \, (\tau - 1)) \, a7 - \sigma \, \omega \, a6 \, \theta \, (D2 \, \beta \, \alpha \, (\tau - 1) \, a5 + \pi \, (\omega \, \tau - \mu - \omega))) \, \beta \, a6 \, a7 \, \theta \, (((D1 \, a1 - a6) \, \theta - D1 \, a1) \, a7 - D2 \, \omega \, \theta \, a6)) \tag{41}$$

$$Z_3 = (\sigma + \mu)(K + \omega + \delta + \mu)(\gamma + \delta + \mu)(\varepsilon + \delta + \mu)(1 - R_0) \tag{42}$$

2.7 Bifurcation Analysis

Theorem 2:

If $R_0 < 1$ and $a_0 = 0$ then the system Eq. (1) to Eq. (7) exhibit a backward at $R_{curve} = 1$. If the inequality holds reversed, then the system exhibits a forward bifurcation at $R_0 = 1$ then

$$\beta_m^* = \frac{(\mu \, (\omega + \mu)(\sigma + \mu)(K + \omega + \delta + \mu)(\gamma + \delta + \mu)(\varepsilon + \delta + \mu))}{\alpha \, \delta \, (\mu + \omega - \tau \, \omega)(D1 \, (1 - \theta)(\mu + \delta + \varepsilon)(K + \omega + \delta + \mu) + \theta \, (\mu + \delta + \varepsilon)(\gamma + \mu + \delta) \, \delta + \theta \, \omega \, D2 \, (\gamma + \mu + \delta) \, \delta)}$$

$$\tag{43}$$

$$\begin{bmatrix} -(\omega+\mu) & 0 & 0 & \dfrac{-\beta_m^*\alpha}{(\omega+\mu)} & \dfrac{-\beta_m^* D_1 \alpha}{(\omega+\mu)} & \dfrac{-\beta_m^* D_2 \alpha}{(\omega+\mu)} & \pi \\[2mm] \omega & -\mu & 0 & \dfrac{-\beta_m^*(1-\tau)\alpha\omega}{\mu(\omega+\mu)} & \dfrac{-\beta_m^* D_1(1-\tau)\alpha\omega}{\mu(\omega+\mu)} & \dfrac{-\beta_m^* D_2(1-\tau)\alpha\omega}{\mu(\omega+\mu)} & 0 \\[2mm] 0 & 0 & -(\sigma+\mu) & \dfrac{\beta_m^*\alpha(\mu+(1-\tau)\omega)}{\mu(\omega+\mu)} & \dfrac{\beta_m^*\alpha D_1(\mu+(1-\tau)\omega)}{\mu(\omega+\mu)} & \dfrac{\beta_m^*\alpha D_2(\mu+(1-\tau)\omega)}{\mu(\omega+\mu)} & 0 \\[2mm] 0 & 0 & \theta\sigma & -(K+\Lambda+\delta+\mu) & 0 & 0 & 0 \\[2mm] 0 & 0 & (1-\theta)\sigma & 0 & -(\gamma+\delta+\mu) & 0 & 0 \\[2mm] 0 & 0 & 0 & \Lambda & 0 & -(\epsilon+\delta+\mu) & 0 \\[2mm] 0 & 0 & 0 & K & \gamma & \epsilon & -(\pi+\mu) \end{bmatrix}$$

From the characteristic equation of the Jacobian matrix: $|J-\lambda I|=0$, we obtained an expression in the form

$$a_4\lambda^4 + a_3\lambda^3 + a_2\lambda^2 + a_1\lambda + a_0 = 0 \tag{44}$$

$$\lambda_1 = C_{11} = (\gamma+\delta+\mu), \lambda_2 = -C_{16} = (\pi+\mu), \lambda_2 = \mu \text{ and}$$

$$\lambda^4 + (C_2 + C_7 + C_{11} + C_{15})\lambda^3 + \big(C_2 C_7 + C_2 C_{11} + C_2 C_{15} - C_3 C_{10} + C_7 C_{11} + C_7 C_{15} + C_{11} C_{15} - (\theta\sigma C_6 + C_3 C_{10})\big)\lambda^2 + \big(C_2 C_{11} C_7 + C_2 C_7 C_{15} + C_2 C_{11} C_{15} + C_7 C_{11} C_{15} - (\theta\sigma C_{14} + \theta\sigma C_6 C_{11} + \theta\sigma C_6 C_{15} + C_3 C_{10} C_{10} + C_3 C_{10} C_{15})\big)\lambda - (\theta\sigma C_{14} C_{11} + \theta\sigma C_6 C_{11} C_{15} + C_3 C_7 C_{10} C_{15}) = 0 \tag{45}$$

$$a_0 = \frac{((1-\theta)\sigma(K+\omega+\delta+\mu)\beta_m^* C1 \alpha(\mu+(1-\tau)\omega)(\varepsilon+\delta+\mu))}{\mu(\omega+\mu)} + \frac{(\omega\theta\sigma C2 \alpha(\mu+(1-\tau)\omega)(\gamma+\delta+\mu))}{(\mu(\omega+\mu))} +$$
$$+ \frac{(\theta\sigma\beta_m^*\alpha(\mu+(1-\tau)\omega)(\gamma+\delta+\mu)(\varepsilon+\delta+\mu))}{(\mu(\omega+\mu))} \tag{46}$$

Hence

$$(\sigma+\mu)(K+\omega+\delta+\mu)(\gamma+\delta+\mu)(\varepsilon+\delta+\mu)(1-R_0) \tag{47}$$

$a_0 = 0$, therefore $(a_4\lambda^4 + a_3\lambda^3 + a_2\lambda^2 + a_1)\lambda = 0$, we can observe that the seven eigen are real and negative and that $\lambda_4 = 0$, now we denote by $w = (w_1, w_2, w_3, w_4, w_5, w_6, w_7)^T$ the right eigen value correspond to $\lambda_4 = 0$.

$$\left.\begin{aligned} w_7\pi - w_1 C_1 - w_4 C_4 - w_5 C_8 - w_6 C_{12} &= 0 \\ -w_2\mu + -w_1\omega - w_4 C_5 - w_5 C_9 - w_6 C_{13} &= 0 \\ -w_3 C_2 + w_4 C_6 + w_5 C_{10} + w_6 C_{14} &= 0 \\ w_3\theta\sigma - w_4 C_7 &= 0 \\ w_3 C_3\sigma - w_5 C_{11} &= 0 \\ w_4\Lambda - w_6 C_{15} &= 0 \\ \epsilon w_6 + \gamma w_5 - w_7 C_{16} + K &= 0 \end{aligned}\right\} \tag{48}$$

Thus at $w_4 = 1$, we have

$$w_1 = \frac{\left(\beta \, \alpha \, (K + \lambda + \delta + \mu) D1 \, (\varepsilon + \delta + \mu) + \theta \, (\gamma + \delta + \mu)\left(\lambda \, D_2 + w_4 \, (\varepsilon + \delta + \mu)\right)\right)}{((\omega + \mu)^2 \theta \, (\gamma + \delta + \mu)(\varepsilon + \delta + \mu))}$$

$$-\frac{((\varepsilon + \delta + \mu) \, (\pi \, K \, \theta \, (\gamma + \delta + \mu) \, (\pi + \mu) + \pi \, \gamma \, (K + \lambda + \delta + \mu)) + \pi \, \lambda \, \varepsilon \, \theta \, (\gamma + \delta + \mu))}{(\theta \, ((\omega + \mu) \, \gamma + \delta + \mu) \, (\pi + \mu) \, (\varepsilon + \delta + \mu))}$$

$$w_2 = \frac{(\beta \, \alpha \, \omega \, (1 - \tau))}{\mu^{\wedge}2} \left(\frac{1}{(\omega + \mu)} + \frac{(D_1 \, (K + \lambda + \delta + \mu))}{(\theta \, (\omega + \mu) \, (\gamma + \delta + \mu))} + \frac{(\lambda \, D_2)}{((\omega + \mu) \, (\varepsilon + \delta + \mu))}\right) - \frac{w_2 \, \omega}{\mu}$$

$$w_3 = \frac{(K + \lambda + \delta + \mu)}{\theta \, \sigma}$$

$$w_5 = \frac{(K + \lambda + \delta + \mu)}{(\theta \, (\gamma + \delta + \mu)}$$

$$w_6 = \frac{\lambda}{(\varepsilon + \delta + \mu)}$$

$$w_7 = K \, + \frac{(\lambda \, \varepsilon)}{(\varepsilon \, (\pi + \mu) + \delta \, (\pi + \mu) + \mu \, (\pi + \mu))} + \frac{\gamma \, (K + \lambda + \delta + \mu)}{\theta \, (\gamma + \delta + \mu) \, (\pi + \mu)}$$

$$\tag{49}$$

The left eigen vector $v = (v_1, v_2, v_3, v_4, v_5, v_6, v_7)$ satisfying $vw = 0$, is given by

$$\left.\begin{array}{r}
\omega v_2 - v_1 C_1 = 0 \\
-v_2 \mu = 0 \\
\theta \sigma v_4 - C_2 v_3 + C_3 v_5 = 0 \\
K v_7 + \Lambda v_6 - C_4 v_1 - C_5 v_2 + C_6 v_3 - C_7 v_4 = 0 \\
\gamma v_7 + C_8 v_1 - C_9 v_2 + C_{10} v_3 - C_{11} v_5 = 0 \\
\epsilon v_7 - C_{12} v_1 - C_{13} v_2 + C_{14} v_3 - C_{15} v_6 = 0 \\
\pi v_1 - C_{16} v_7 = 0
\end{array}\right\} \tag{50}$$

$$\left.\begin{array}{l}
v_1 = v_2 = v_7 = 0, \; v_4 = 1 \\
v_3 = \dfrac{((\gamma + \delta + \mu) \, \theta \, \sigma \, \mu \, (\omega + \mu))}{(\mu \, (\omega + \mu) \, (\gamma + \delta + \mu) \, (\sigma + \mu) + D1 \, \sigma \, \alpha \, \beta \, (\mu + (1 - \tau) \, \omega) \, (1 - \theta))} \\
v_5 = \dfrac{(\beta \, \alpha \, D1 \, (\mu + (1 - \tau) \, \omega) \, \theta \, \sigma)}{(\mu \, (\sigma + \mu) \, (\gamma + \delta + \mu) \, (\omega + \mu) + \beta \, \alpha \, D_1 \, (1 - \theta) \, (\mu + (1 - \tau) \, \omega))} \\
v_6 = \dfrac{\left(\beta^2 D_2{}^2 \sigma \, (\mu + (1 - \tau)\omega)\theta^2 \alpha^2\right)}{((\omega + \mu) \, (\varepsilon + \delta + \mu) \, (\mu \, (\omega + \mu) \, (\gamma + \delta + \mu) \, (\sigma + \mu) - \beta \, (\mu + (1 - \tau) \, \omega)(1 - \theta) \, \alpha \, D_1))}
\end{array}\right\} \tag{51}$$

From the bifurcation process, we have to compute A and B, where

$$A = \sum_{k,i,j=1}^{n} v_k w_i w_j \frac{\partial^2}{\partial x_i \partial x_j} f_k \text{ and } A = \sum_{k,i,j=1}^{n} v_k w_i \frac{\partial^2}{\partial x_i \partial x_\beta} f_k. \tag{52}$$

Let $x_1 = S, x_2 = V, x_3 = E, x_4 = I, x_5 = A, x_6 = Q$ and $x_7 = R$.
Since $v_1 = v_2 = v_7 = 0$, then

$$v_3 \sum_{i,j=1}^{7} w_i w_j \frac{\partial^2 f_3}{\partial x_i \partial x_j} + v_5 \sum_{i,j=1}^{7} w_i w_j \frac{\partial^2 f_5}{\partial x_i \partial x_j} + v_6 \sum_{i,j=1}^{7} w_i w_j \frac{\partial^2 f_6}{\partial x_i \partial x_j} + \sum_{i,j=1}^{7} w_i w_j \frac{\partial^2 f_4}{\partial x_i \partial x_j} \tag{53}$$

$$v_5 \sum_{i,j=1}^{7} w_i w_j \frac{\partial^2 f_5}{\partial x_i \partial x_j} = v_6 \sum_{i,j=1}^{7} w_i w_j \frac{\partial^2 f_6}{\partial x_i \partial x_j} = \sum_{i,j=1}^{7} w_i w_j \frac{\partial^2 f_4}{\partial x_i \partial x_j} = 0 \tag{54}$$

Therefore

$$2v_3 \left(w_1 w_4 \frac{\partial^2 f_3}{\partial x_1 \partial x_4} + w_1 w_5 \frac{\partial^2 f_3}{\partial x_1 \partial x_5} + w_1 w_6 \frac{\partial^2 f_3}{\partial x_1 \partial x_6} + w_2 w_4 \frac{\partial^2 f_3}{\partial x_2 \partial x_4} + w_2 w_5 \frac{\partial^2 f_3}{\partial x_2 \partial x_5} + w_2 w_6 \frac{\partial^2 f_3}{\partial x_2 \partial x_6}\right) \tag{55}$$

$$f_3 = \beta (D_1 x_5 + D_2 x_6 + x_4)x_1 + \beta (1 - \tau) (D_1 x_5 + D_2 x_6 + x_4) x_2 - (\sigma + \mu) x_3 \qquad (56)$$

We have the following expressions

$$\frac{\partial^2 f_3}{\partial x_1 \partial x_4} = \beta, \frac{\partial^2 f_3}{\partial x_1 \partial x_5} = \beta D_1, \frac{\partial^2 f_3}{\partial x_1 \partial x_6} = \beta D_2, \frac{\partial^2 f_3}{\partial x_2 \partial x_4} = \beta (1 - \tau), \frac{\partial^2 f_3}{\partial x_2 \partial x_5} = \beta (1 - \tau)D_1 \text{ and}$$

$$\frac{\partial^2 f_3}{\partial x_2 \partial x_6} = \beta (1 - \tau)D_1 \qquad (57)$$

Also

$$\frac{\partial^2 f_3}{\partial x_4 \partial x_\beta} = x_1(1 - \tau)x_2, \frac{\partial^2 f_3}{\partial x_5 \partial x_\beta} = D_1 x_1 + (1 - \tau)D_1 x_2, \frac{\partial^2 f_3}{\partial x_6 \partial x_\beta} = D_1 x_1 + (1 - \tau)D_1 x_2 \qquad (58)$$

All the remain partial derivatives are zero, hence we have

$$A = \frac{2 \beta \theta \sigma \mu (\delta + \gamma + \mu) (\mu + \omega)}{(\mu (\mu + \omega) (\delta + \gamma + \mu) (\sigma + \mu) + D1 \sigma \alpha \beta (\mu + (1 - \tau) \omega) (1 - \theta))} M_1 \qquad (59)$$

$$M_1 = \left(\frac{(K + \Lambda + \delta + \mu) D_1}{\theta (\gamma + \delta + \mu)} + \frac{D_2 \Lambda}{\varepsilon + \delta + \mu} + w_4 \right) (w_1 + (1 - \tau) w_2) \qquad (60)$$

$$B = \frac{(\alpha \theta \sigma (D1 + D2 + 1) (-\omega \tau + \mu + \omega) (\gamma + \delta + \mu))}{(\mu (\omega + \mu) (\gamma + \delta + \mu) (\sigma + \mu) + D1 \sigma \alpha \beta (\mu + (1 - \tau) \omega) (1 - \theta))} M_2 \qquad (61)$$

$$M_2 = w_1 + \frac{(\beta \alpha \omega (1 - \tau))}{\mu^2} \left(\frac{1}{(\omega + \mu)} + \frac{D_1 (K + \Lambda + \delta + \mu)}{(\theta (\omega + \mu) (\gamma + \delta + \mu))} + \frac{D_2 \Lambda}{(\omega (\varepsilon + \delta + \mu) + \mu (\varepsilon + \delta + \mu))} \right) +$$
$$\frac{(K + \Lambda + \delta + \mu)}{\theta \sigma} + w_4 + \frac{K + \Lambda + \delta + \mu}{\theta (\gamma + \delta + \mu)} + \frac{\Lambda}{\varepsilon + \delta + \mu} + K + \frac{\Lambda \varepsilon}{\varepsilon (\pi + \mu) + \delta (\pi + \mu) + \mu (\pi + \mu)} + \frac{K + \Lambda + \delta + \mu}{\theta (\gamma + \delta + \mu) (\pi + \mu)} -$$
$$\frac{w_1 \omega}{\mu} \qquad (62)$$

Since the coefficient of B is always positive, its the sign of the coefficient of A (M_1) which decides the local dynamics around the disease-free equilibrium at $\beta = \beta^*$, if the coefficient is positive then the direction of the bifurcation is backward otherwise its forward. EEP is both locally and globally asymptomatically stable when $R_0 > 1$, while DFE is locally asymptotically stable when $R_0 < 1$ but it's not globally asymptotically stable when $R_0 < 1$

Figures 2 to 4 depict the influence of vaccine efficacy on the bifurcation diagram. As vaccine efficacy increases, a noticeable transformation occurs in the bifurcation diagram, shifting it from a backward pattern to a forward one.
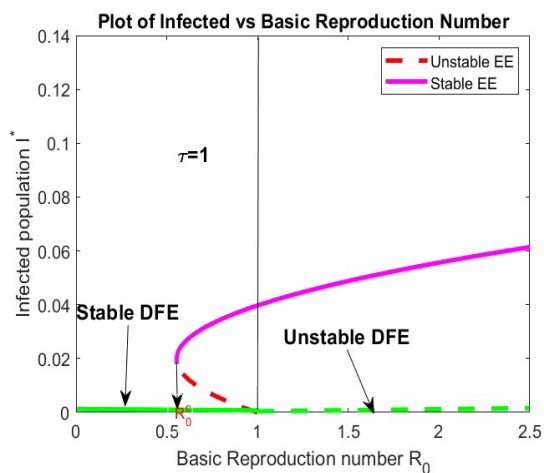
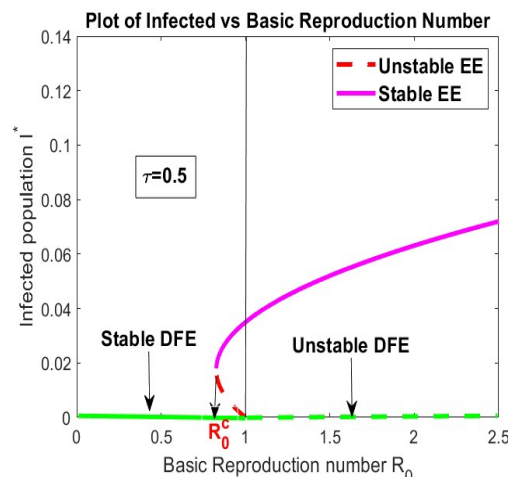**Fig. 2.** Infected versus basic reproduction number at $\tau = 1$

Fig. 3. Infected versus basic reproduction number at $\tau = 0.5$
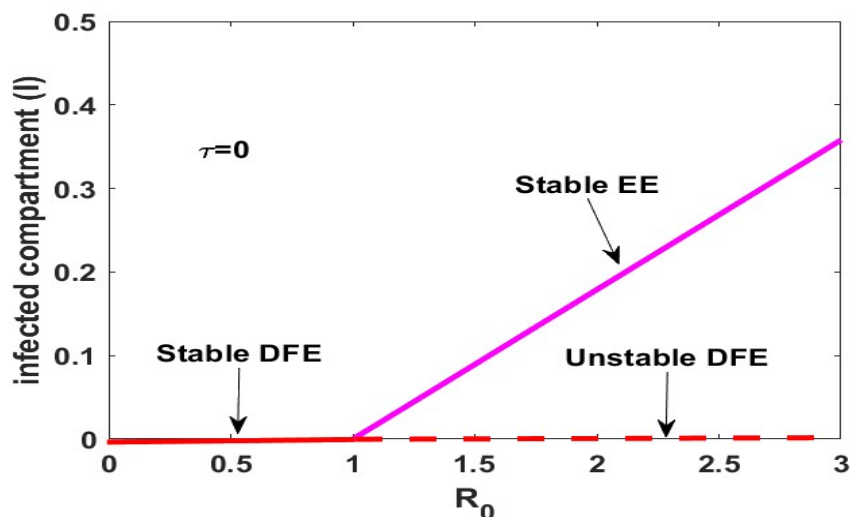

Fig. 4. Infected versus basic reproduction number at $\tau = 0.0$

3. Global Stability of the Endemic Equilibrium

Theorem 3: if $R_0 > 1$, the endemic equilibrium E_0 of the model is globally asymptotically stable.

Proof: By Lyapunov's direct method and Lasale's invariant principle [15,16], we prove the above theorem by defining a Lyapunov's function

$$L(S^*, V^*, E^*, I^*, A^*, Q^*, R^*) = \left(S - S^* - S^* \ln \frac{S^*}{S}\right) + \left(V - V^* - V^* \ln \frac{V^*}{V}\right) + \left(E - E^* - E^* \ln \frac{E^*}{E}\right) +$$
$$\left(A - A^* - A^* \ln \frac{A^*}{A}\right) + \left(Q - Q^* - Q^* \ln \frac{Q^*}{Q}\right) + \left(I - I^* - I^* \ln \frac{I^*}{I}\right) + \left(R - R^* - R^* \ln \frac{R^*}{R}\right) \quad (63)$$

Differentiating L with respect to t and substituting the values of $\frac{dS}{dt}, \frac{dV}{dt}, \frac{dE}{dt}, \frac{dI}{dt}, \frac{dA}{dt}, \frac{dQ}{dt}, \frac{dR}{dt}$ into $\frac{dL}{dt}$ and then simplify to get

$$\frac{dL}{dt} = \alpha + \frac{S^*}{S}(\lambda + \omega\mu)S + \frac{V^*}{V}\left((1-\tau)\lambda + \mu\right)V + \frac{E^*}{E}(\sigma + \mu)E + \frac{I^*}{I}(K + \omega + \delta + \mu)I +$$

$$\sigma E + \frac{A^*}{A}(\gamma + \delta + \mu)A + \frac{Q^*}{Q}(\varepsilon + \delta + \mu)Q + \frac{R^*}{R}(\pi + \mu)R - \left(\mu S + \frac{S^*}{S}\alpha + \frac{S^*}{S}\pi R + \mu V +\right.$$

$$+\frac{V^*}{V}\omega S + (\sigma + \mu)E + \frac{E^*}{E}\lambda S + \frac{E^*}{E}(1-\tau)\lambda V + (\delta + \mu)I + \frac{I^*}{I}\theta\sigma E + (\delta + \mu)A + \frac{A^*}{A}(1 -$$

$$\left.\theta)\sigma E + (\delta + \mu)Q + \frac{Q^*}{Q}\omega I + \mu R + \beta_0 \right) \tag{64}$$

Which can be written as

$$\frac{dL}{dt} = \Im_1 - \Im_2 \tag{65}$$

$$\beta_0 = \frac{R^*}{R}KI + \frac{R^*}{R}\gamma A + \frac{R^*}{R}\epsilon Q \tag{66}$$

$$\frac{dL}{dt} \leq 0 \; iff \; \Im_1 < \Im_2 \tag{67}$$

$\frac{dL}{dt} = 0$ if and only if $S = S^*, V = V^*, E = E^*, I = I^*, A = A^*, Q = Q^*, R = R^*$ Therefore, the largest invariant set in $\{(S^*, V^*, E^*, I^*, A^*, Q^*, R^*) \in \Omega\}$ is the singleton set E_0^* where E* 0 is the endemic equilibrium of the system (1). Therefore, by Lasalle's Invariant principle, it implies that E_0^* is globally asymptotically stable in Ω if $\Im_1 < \Im_2$.

3.1 Global Stability of Threshold Analysis and Effect of Imperfect Vaccine

Given that we considered the HFMD vaccination was flawed, it is instructive to assess whether or not widespread use in a community is constantly assured.

To measure the effect of such a vaccine on disease transmission, a qualitative approach can be utilized as discussed in [19-24] by differentiating the expression R_0 with respect to the fraction of individuals immunized at the steady state and permitting

$$\theta_* = \frac{V^*}{N_*} \tag{68}$$

As a result, θ_* can be regarded as a variable that decides R_0 therefore

$$R_0 = R_0(\theta_*) = R_0(1 - \tau\theta_*) \tag{69}$$

Observing that $R_0 \leq R_b$ if $\omega = 0$, i.e., $\theta_0 = 0$ or $\tau = 0$, That is to say, even if the vaccine does not work effectively, it is essential to note that as the rate of infection declines, so will the spread of the disease. With $\omega > 0$ and $\tau > 0$ illness's effect would be reduced. As a result, the prerequisite for θ_* is equally critical and sufficient for control, just as $R_0 \leq 1$ is a necessary and sufficient condition for disease elimination.

$$\theta_* \geq \frac{1}{\tau}\left(1 - \frac{1}{R_b}\right) = \theta_\Lambda \tag{70}$$

Combining the information from bifurcation analysis with theorem 3 yields the desired outcome.

Lemma 2: HFMD is removable from the population if $\theta_* > \theta_\Lambda$. Our definition of the percentage vaccinated at equilibrium point θ_Λ is the same as that found in [19]. Figure 5 depicts the crucial value, θ_Λ, as a function of τ for a variety of R_0 values. According to Eq. (70), both the vaccinated fraction, θ and vaccine efficacy, τ play important roles in reducing R_0, and both must be high in order to reduce the value of R_0 to less than one and thereby manage the disease. Inequality can be confirmed as well.

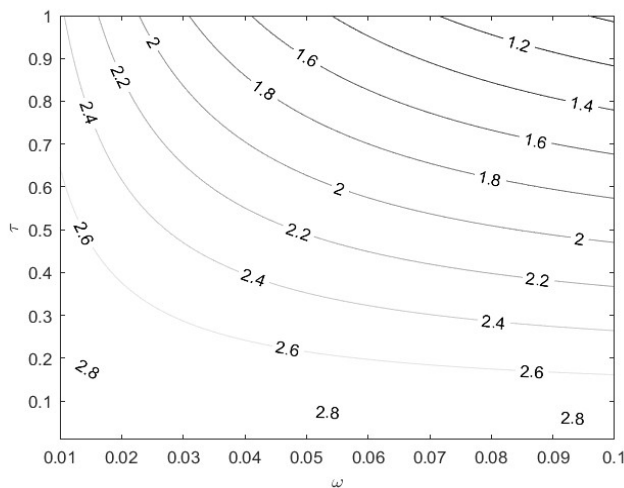$$\theta_* \tau \geq \frac{1}{\tau}\left(1 - \frac{1}{R_b}\right) \tag{71}$$

Fig. 5. Contour plot of the basic reproductive number as a function of vaccine efficacy

3.2 Estimation of Parameters

The SVEIAQR model takes into account weekly fluctuations in government-imposed travel restrictions and lockdown circumstances in Malaysia in 2021 due to COVID 19, Data were gathered from [17,18] sources, estimated and incorporated into the model as functions of (t) and $I(t)$. We obtained time-series data on the number of infections, and positive rate for Sarawak in Malaysian for the year 2021, from the ministry of economy department of statistics Malaysia official portal (https://www.dosm.gov.my/portal-main/landingv2).

Table 1
Summary of the parameter's values

Parameters	Values	Reference
α	0.0002923000	[18]
μ	0.0001077000	[18]
D_1	0.0000400000	Assume
D_2	0.0000600000	Assume
ω	0.0001010101	Assume
Λ	0.0001010101	Assume
γ	0.0001000000	[17]
θ	0.5000000000	Data fitting
δ	0.0001731000	[18]
β	0.0000300000	[18]
τ	0.0001010101	Assume
ϵ	0.1000000000	[17]
π	0.1000000000	[18]

σ	0.1042308906	Data fitting
I_0	53.371777754	Data fitting
E_0	4.786108e+03	Data fitting
A_0	8.267797e+05	Data fitting
R_0	4.5329e-14	

Figure 6 illustrates a Comparison Graph showcasing the Hand, Foot, and Mouth Disease (HFMD) data from Sarawak, Malaysia, alongside the simulation outcomes generated by Model Eq. (1) to Eq. (7). This visual representation offers a valuable comparison between the actual HFMD data and the predictions produced by the mathematical model. By presenting real-world observations alongside modelled results, Figure 6 provides insights into the model's performance and its ability to replicate observed trends. This figure plays a crucial role in validating the model's accuracy and in assessing its capacity to simulate HFMD dynamics in the Sarawak region.
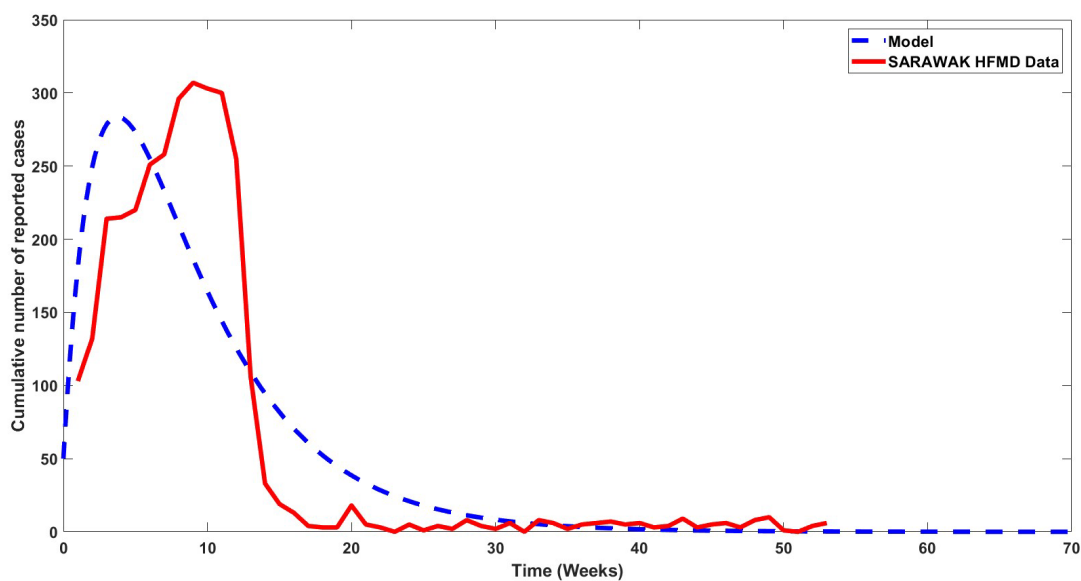

Fig. 6. The Comparison Graph of HFMD data in Sarawak (Malaysia) and Simulation Results by Model Eq. (1) to Eq. (7)

4. Results
4.1 Graphical Representation

This section discusses the graphical results obtained from the model equations and the parameters. The effects of K, τ and π are discussed in the next sub section.

The graphical solution depicting the rates of exposure to infected (σ), infected to recovery (K), and recovery to susceptible (π) provides a dynamic insight into the disease transmission and recovery processes.

   i.   **Infected to Recovery Rate** (K)**:** Figure 7 and 8 demonstrates the pace at which infected individuals recover and transition to the recovered state. As K increases, it signifies a swifter recovery process, reducing the number of infected individuals and contributing to the overall control of the disease spread. The curve's behaviour reflects the interplay between recovery rates, medical interventions, and the immune response.

  ii.   **Rate of Exposure to Infected** (σ)**:** Figure 10 illustrates how the rate of individuals transitioning from the susceptible state to the exposed state is influenced by factors such

as contact rates and transmission probabilities. As the values of σ rises, it indicates an increase in the rate at which individuals become exposed to the disease due to interactions with infected individuals. This rate becomes a critical determinant in shaping the course of an outbreak.

iii. **Recovery to Susceptible Rate** (π): The graph of the recovery rate (Figure 9.) provides a visual representation of how quickly infected individuals transition to the recovered state. It showcases the impact of medical interventions, immune responses, and other factors influencing recovery time. As the recovery rate increases, the infected population reduces, indicating a faster resolution of infections. This graph is essential in understanding the effectiveness of treatments and the potential to control disease spread. It offers valuable insights into the temporal dynamics of recovery within a population and guides strategies for managing outbreaks and minimizing the impact of infectious diseases.

iv. By visualizing these rates collectively, the graphical solution underscores the intricate balance between exposure, recovery, and immunity within the population. This dynamic perspective aids in comprehending the interdependencies that govern disease transmission and informs public health interventions aimed at mitigating outbreaks.
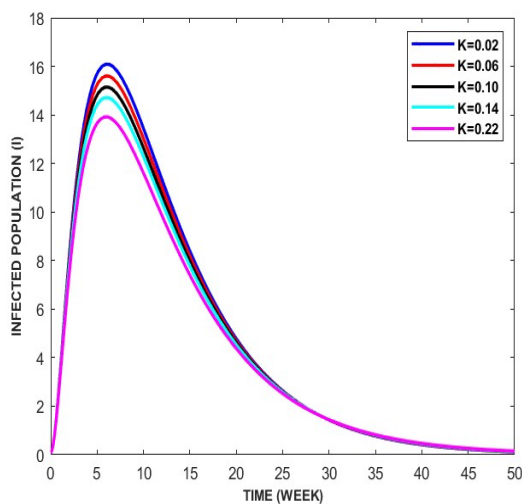

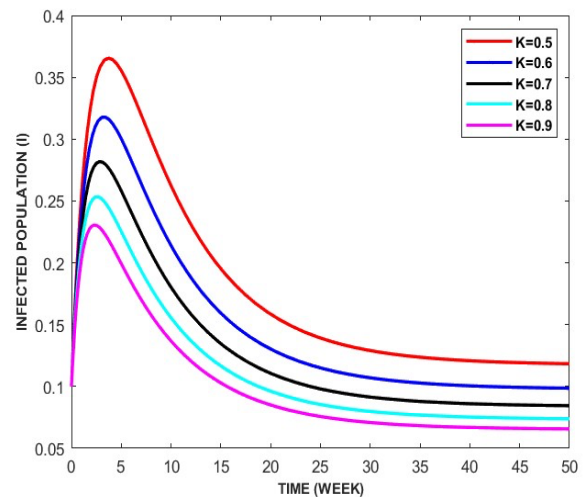**Fig. 7.** Graph of Infected Population at different values of K

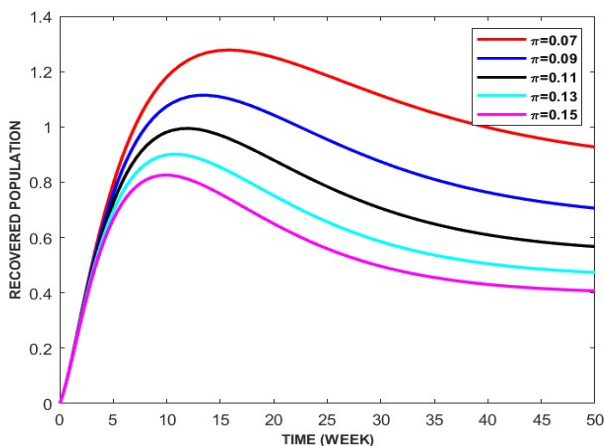**Fig. 8.** Graph of Infected Population at different values of K

Fig. 9. Graph of Recover Population at different values of π
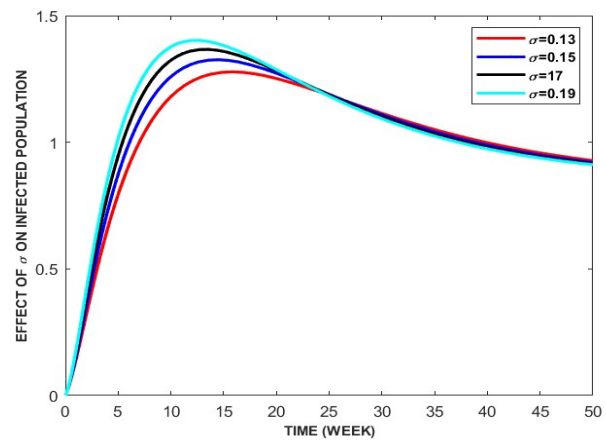

Fig. 10. Effect of σ on infected Population

5. Conclusions

From the given model equation and the data provided, we were able to simulate the dynamics of the infectious disease and estimate the values of the parameters using curve fitting. The analysis showed that the model exhibits a backward bifurcation, indicating that increasing the vaccination rate alone may not be sufficient to eliminate the disease.

To effectively control the disease, a combination of control strategies, including vaccination, quarantine, and increasing public awareness through education, should be implemented. The control strategy should aim to reduce the basic reproduction number to below 1, thereby achieving disease elimination.

The objective of the control strategy should be to minimize the number of infected individuals, reduce the impact of the disease on public health and the economy, and prevent future outbreaks. To achieve these objectives, there should be effective coordination and collaboration between public health officials, policymakers, and the public.

In conclusion, the analysis highlights the importance of a multi-faceted approach to disease control and the need for accurate data and modelling to inform decision-making.

References
[1] Liu, Junli. "Threshold dynamics for a HFMD epidemic model with periodic transmission rate." *Nonlinear Dynamics* 64 (2011): 89-95. https://doi.org/10.1007/s11071-010-9848-6

[2] Schmidt, Nathalie J., Edwin H. Lennette, and Helen H. Ho. "An apparently new enterovirus isolated from patients with disease of the central nervous system." *Journal of infectious diseases* 129, no. 3 (1974): 304-309. https://doi.org/10.1093/infdis/129.3.304

[3] Aswathyraj, S., G. Arunkumar, E. K. Alidjinou, and D. Hober. "Hand, foot and mouth disease (HFMD): emerging epidemiology and the need for a vaccine strategy." *Medical microbiology and immunology* 205 (2016): 397-407. https://doi.org/10.1007/s00430-016-0465-y

[4] Ho, Monto. "Enterovirus 71: the virus, its infections and outbreaks." *Journal of Microbiology, Immunology, and Infection= Wei Mian yu gan ran za zhi* 33, no. 4 (2000): 205-216.

[5] Huang, Zehong, Mingzhai Wang, Luxia Qiu, Ning Wang, Zeyu Zhao, Jia Rui, Yao Wang *et al.,* "Seasonality of the transmissibility of hand, foot and mouth disease: a modelling study in Xiamen City, China." *Epidemiology & Infection* 147 (2019): e327. https://doi.org/10.1017/S0950268819002139

[6] Chan, L. G., Umesh D. Parashar, M. S. Lye, F. G. L. Ong, Sherif R. Zaki, James P. Alexander, K. K. Ho *et al.,* "Deaths of children during an outbreak of hand, foot, and mouth disease in Sarawak, Malaysia: clinical and pathological characteristics of the disease." *Clinical infectious diseases* 31, no. 3 (2000): 678-683. https://doi.org/10.1086/314032

[7] Coates, Sarah J., Mark DP Davis, and Louise K. Andersen. "Temperature and humidity affect the incidence of hand, foot, and mouth disease: a systematic review of the literature–a report from the International Society of Dermatology Climate Change Committee." *International journal of dermatology* 58, no. 4 (2019): 388-399. https://doi.org/10.1111/ijd.14188

[8] Shi, Lei, Hongyong Zhao, and Daiyong Wu. "Modelling and analysis of HFMD with the effects of vaccination, contaminated environments and quarantine in mainland China." *Mathematical Biosciences and Engineering* 16, no. 1 (2019): 474-500. https://doi.org/10.3934/mbe.2019022

[9] Dolin, Raphael. "Enterovirus 71—emerging infections and emerging questions." *New England Journal of Medicine* 341, no. 13 (1999): 984-985. https://doi.org/10.1056/NEJM199909233411309

[10] Chowell, Gerardo, and Hiroshi Nishiura. "Transmission dynamics and control of Ebola virus disease (EVD): a review." *BMC medicine* 12 (2014): 1-17. https://doi.org/10.1186/s12916-014-0196-0

[11] Qiu, Jane. "Enterovirus 71 infection: a new threat to global public health?." *The Lancet Neurology* 7, no. 10 (2008): 868-869. https://doi.org/10.1016/S1474-4422(08)70207-2

[12] Liew, Chin Ying, Nor Shamira Sabri, Boon Hao Hong, and Jane Labadin. "Exploring Bipartite Network Approach in Hand, Foot and Mouth Disease Hotspot Identification." *Journal of Smart Science and Technology* 3, no. 1 (2023): 25-36. https://doi.org/10.24191/jsst.v3i1.39

[13] Mahardika, R., Widowati, and Y. D. Sumanto. "Routh-hurwitz criterion and bifurcation method for stability analysis of tuberculosis transmission model." In *Journal of physics: Conference series*, vol. 1217, no. 1, p. 012056. IOP Publishing, 2019. https://doi.org/10.1088/1742-6596/1217/1/012056

[14] Castillo-Chavez, Carlos, Sally Blower, Pauline van den Driessche, Denise Kirschner, and Abdul-Aziz Yakubu, eds. *Mathematical approaches for emerging and reemerging infectious diseases: models, methods, and theory*. Vol. 126. Springer Science & Business Media, 2002. https://doi.org/10.1007/978-1-4613-0065-6

[15] LaSalle, Joseph P. "Stability theory and invariance principles." In *Dynamical systems*, pp. 211-222. Academic Press, 1976.

[16] Rwat, Solomon Isa, and Noor Atinah Ahmad Ahmad. "Backward Bifurcation and Hysteresis in a Mathematical Model of COVID19 with Imperfect Vaccine." *MATEMATIKA: Malaysian Journal of Industrial and Applied Mathematics* (2023): 87-99. https://doi.org/10.11113/matematika.v39.n1.1458

[17] Li, Yong, Jinhui Zhang, and Xinan Zhang. "Modeling and preventive measures of hand, foot and mouth disease (HFMD) in China." *International journal of environmental research and public health* 11, no. 3 (2014): 3108-3117. https://doi.org/10.3390/ijerph110303108

[18] Chan, Sze Jan, Jane Labadin, and Yuwana Podin. "A dynamic SEIPR model for the spread of hand, foot and mouth disease in Sarawak." *Journal of Telecommunication, Electronic and Computer Engineering (JTEC)* 9, no. 3-10 (2017): 125-129.

[19] Duan, Xichao, Sanling Yuan, Zhipeng Qiu, and Junling Ma. "Global stability of an SVEIR epidemic model with ages of vaccination and latency." *Computers & Mathematics with Applications* 68, no. 3 (2014): 288-308. https://doi.org/10.1016/j.camwa.2014.06.002

[20] Feng, Zhilan, Sherry Towers, and Yiding Yang. "Modeling the effects of vaccination and treatment on pandemic influenza." *The AAPS journal* 13 (2011): 427-437. https://doi.org/10.1208/s12248-011-9284-7

[21] Lai, C-C., D-S. Jiang, H-M. Wu, and H-H. Chen. "A dynamic model for the outbreaks of hand, foot, and mouth disease in Taiwan." *Epidemiology & Infection* 144, no. 7 (2016): 1500-1511. https://doi.org/10.1017/S0950268815002630

[22] Sabastine Emmanuel, Saratha Sathasivam, Majid Khan Majahar Ali, TJ Kee, YS Ling. "Estimating The Transmission Dynamics Of Dengue Fever In Subtropical Malaysia Using SEIR Model" *Journal of Quality Measurement and Analysis* 19, no. 2(2023): 45-56. https://journalarticle.ukm.my/22244/1/Paper4%20-.pdf

[23] Agoeng, Chandra, Nurul Dini Faqriah Miza Azmi, Hakimah Mat Harun, Nurzulaikha Abdullah, Wan Azani Mustafa, and Fakhitah Ridzuan. "Leveraging Correlation and Clustering: An Exploration of Data Scientist Salaries." *Journal of Advanced Research in Computing and Applications* 35, no. 1 (2024): 10-20. https://doi.org/10.37934/arca.35.1.1020

[24] Zulkefli, Nor Atirah Izzah, Yeak Su Hoe, and Nor Afifah Hanim Zulkefli. "Fuzzy Predator-Prey Systems by Extended Runge-Kutta Method with Polynomial Interpolation Technique." *Semarak International Journal of Machine Learning* 1, no. 1 (2024): 11-19.

Name	Email
Putsadee Pornphol	putsadee.p@pkru.ac.th
Porpattama Hammachukiattikul	porpattama@pkru.ac.th
Rajarathinam Vadivel	vadivelsr@yahoo.com
Emmanuel Sabastine	sabastine.emmanuel@fulokoja.edu.ng
Saratha Sathasivam	saratha@usm.my